Preliminary results of the 2001-2002 Gemini sodium monitoring campaign at Cerro Tololo, Chile

Céline d'Orgeville*[a], Francois Rigaut[a], Maxime Boccas[a], Chris Dainty[†b], Enrique Figueroa[d], Ralf Flicker[††c], Brooke Gregory[‡d], Laurent Michaille[b], John Quartel[b], Andrei Tokovinin[d], Gelys Trancho[a], Nick Wooder[b]
[a]Gemini Observatory; [b]Blackett Laboratory, Imperial College; [c]Lund Observatory; [d]Cerro Tololo Inter-American Observatory

ABSTRACT

In the near future several astronomical observatories in Chile are planning to use sodium laser guide stars to increase the sky coverage provided by their adaptive optics facilities. Knowledge of the mesospheric sodium layer behavior is crucial to predict the performance of future laser guide star adaptive optics systems. Whereas the sodium layer has been observed quite extensively at several locations, many of them in the Northern Hemisphere, very little measurements have been made in Chile. The Gemini Observatory therefore initiated a year-long sodium monitoring campaign at the Cerro Tololo Inter-American Observatory located only a few kilometers away from the Gemini South telescope where a conventional laser guide star facility will be offered to the community in 2005, soon to be upgraded to a multi-conjugate adaptive optics system with five laser guide stars. This paper reports on the laser-based sodium monitoring experimental set up and data reduction techniques, and presents some preliminary results on the sodium column density and layer altitude variations observed from February 2001 to February 2002. Implications for the Gemini South Adaptive Optics system expected performance are presented as well.

Keywords: mesospheric sodium layer, column density, laser guide star adaptive optics

1. INTRODUCTION

1.1. Mesospheric sodium layer

The layer of sodium atoms that exists about 90km high up in the mesosphere has been of interest to atmosphere scientists long before astronomers came up with their idea to create artificial stars by exciting sodium atoms with a laser for adaptive optics[1]. Large amounts of data have been collected in the past 30 years that describe the mesospheric sodium layer behavior and provide grounds to study its physics. Sodium atoms are believed to be deposited in the high atmosphere by meteoritic ablation. They form a layer whose average altitude lies in the 90-95km altitude range above sea level, and can extend from 85 to 105km high. One of the most abundant metallic layer in the mesosphere, the sodium layer has column densities in the 1 to 10 10^9 atoms/cm^2 range. Extensive data are available in the literature and on the web[2] for Northern and Southern[3] hemisphere latitudes that indicate significant abundance variations on hourly, daily and yearly time scales. Up to 10-fold variations have been reported on time scales of a few minutes to a few hours while typical seasonal variations are on the order of a factor of 2 to 4. The sodium layer mean altitude and width also exhibit significant variations on short and long time scales. Sodium abundance usually reaches its minimum in summer time and maximum in winter time, while the layer is in average lower in altitude (by 1 to 2km) and thinner (by ~1km) at the equinoxes, and higher in altitude and thicker at the solstices[4]. Most of the short time scale abundance and mean altitude variations can be traced down to the appearance of relatively short-lived, high density, thinner layers within the main sodium layer, which are subsequently called "sporadics". The observation of sporadic layers has triggered a number of theories aimed at explaining the physics behind these events. Several explanations have been proposed,

---

*cdorgeville@gemini.edu; phone +1 808 974 2545; fax +1 808 935 9235; http://www.gemini.edu; Gemini Observatory, University Park, 670 N. A'Ohoku Place, Hilo HI 96720, USA; [†]c.dainty@ic.ac.uk; phone +44 20 7594 7712; fax +44 20 7594 7714; http://www.photonics.ic.ac.uk; Blackett Laboratory, Imperial College, London SW7 2BZ, UK; [††]ralf@astro.lu.se; Lund Observatory, Box 43, SE-22100 Lund, Sweden; [‡]bgregory@ctio.noao.edu; http://www.ctio.noao.edu; Cerro Tololo Inter-American Observatory, Casilla 603, La Serena, Chile

involving winds, temperature, gravity waves, direct meteor deposition, coupling with *E* layers, redistribution of the background sodium layer, release from aerosol particles, neutral and ion chemistry, etc[5, 6]. In particular, a significant number of observations suggests a possible latitude dependence governing the frequency of sporadic events at a given latitude[7, 8].

Knowledge of the mesospheric sodium layer behavior is crucial to predict the performance of laser guide star adaptive optics systems. However very few data have been published about the mesospheric sodium content above Chile where major astronomical observatories are planning to use sodium laser guide stars in order to increase the sky coverage provided by their adaptive optics facilities. Spectroscopic observations of nearby (<50pc) early type unreddened stars for the benefit of the European Southern Observatory (ESO) provided a few data points for sodium abundance at 29°S latitude in La Silla[9], but the limited number of hours dedicated to this program and the long exposure times necessary to achieve usable signal to noise ratios did not yield much information on short-time scales and seasonal abundance variations. Besides, the spectroscopic technique yielded no information at all on the sodium layer altitude nor did it report on sporadic events. A complete characterization of the sodium layer parameters was therefore needed to plan for future sodium LGS AO systems such as the Gemini South adaptive optics facility[10]. Instead of the spectroscopic technique, we proposed to use the laser-based sodium monitoring technique developed by the Imperial College for their sodium monitoring campaign at the Observatorio del Roque de Los Muchachos in the Canarian Island of La Palma[11, 12].

The program described in this paper arose from a collaboration between the Gemini Observatory, the Imperial College, the Cerro Tololo Inter-American Observatory (CTIO), the AURA New Initiative Office (NIO) and the European Southern Observatory (ESO), all organizations which have a common interest in the technique and achievable performance of sodium laser guide star adaptive optics. It made sense for the Gemini Observatory to study the mesospheric sodium content as close as possible to their Southern telescope where a multi-sodium laser guide star multi-conjugate adaptive optics system is planned in the next few years[10]. Therefore telescopes on Cerro Tololo, only a few kilometers away from Cerro Pachon, were a logical choice to run the experiment. The Gemini Observatory initiated the collaboration among the various institutions, requested and obtained the necessary telescope time at CTIO, coordinated logistics, prepared and ran the experiment, and is now performing data-reduction. The Imperial College loaned most of the experimental hardware and contributed the expertise that was gained during the La Palma sodium monitoring campaign[11, 12]. The Cerro Tololo Inter-American Observatory provided infrastructure for the laser room and telescopes as well as on-site technical support, while the AURA New Initiative Office and ESO supported part of the cost of the experiment.

1.2. CTIO sodium monitoring campaign

The technique that we used was developed by the Imperial College for the la Palma sodium monitoring campaign[11, 12]. It consists in launching a laser beam whose wavelength is tuned to the sodium D2 absorption line to the sky in order to excite mesospheric sodium atoms and imaging the artificial sodium star thus created. Fluorescing atoms in the sodium layer that are distributed along the laser beam appear as a streak on the CCD of a distant telescope (see Figure 1). The intensity profile along the laser star elongated image gives direct information on the sodium abundance distribution versus altitude. The further the telescope, the more elongated the streak appears. The streak must not be stretched too much so that sufficient signal to noise ratio (SNR) per pixel is preserved. Distance of the telescope to the launch location, CCD pixel size and typical laser star widths obtained on the sky dictate the choice of the telescope which is best suited to obtain good spatial resolution on the sky. The telescope diameter then sets the lower limit to exposure times achievable with reasonable SNR. In our experiment, sodium atoms are excited with a low-power continuous-wave laser whose interaction with the atoms is well-known[13]. Provided that all due telescope calibrations are performed and that the atmosphere optical transparency is measured during the night, the CCD data contains all information necessary to retrieve the sodium column density, sodium layer width and relative altitude. Observation of the laser star with an auxiliary telescope is desirable to derive higher accuracy on the sodium layer absolute altitude. Synchronization of exposures between the two observing telescopes enables the use of a passing star trail beginning or end location on the CCD cameras to derive the absolute altitude by triangulation. Figure 1 gives a schematic of the laser technique and presents the particular geometry of the experimental set-up reported below.

Observations were spread over one year from February 2001 to February 2002 to allow characterization of hourly, nightly and yearly variations of the sodium layer parameters. We requested and obtained telescope time at the CTIO

0.9m and University of Michigan Schmidt telescopes with 5 runs of 7 to 10 nights during bright time in February, May, September, November 2001 and February 2002. Those particular months were chosen to match the expected maximum (Nov./Dec.) and minimum (May) of the sodium column density sinusoid-like variations which are presented in reference[4]. Table 1 below indicates the dates of each run, the number of nights when data were taken (sometimes through clouds), and among those the number of clear weather nights usable for sodium abundance computation. Apart from run #2 for which the nights of May 17-20, 2001 were only half nights at the Schmidt telescope, we were always granted simultaneous telescope time on the 0.9m and Schmidt telescopes.

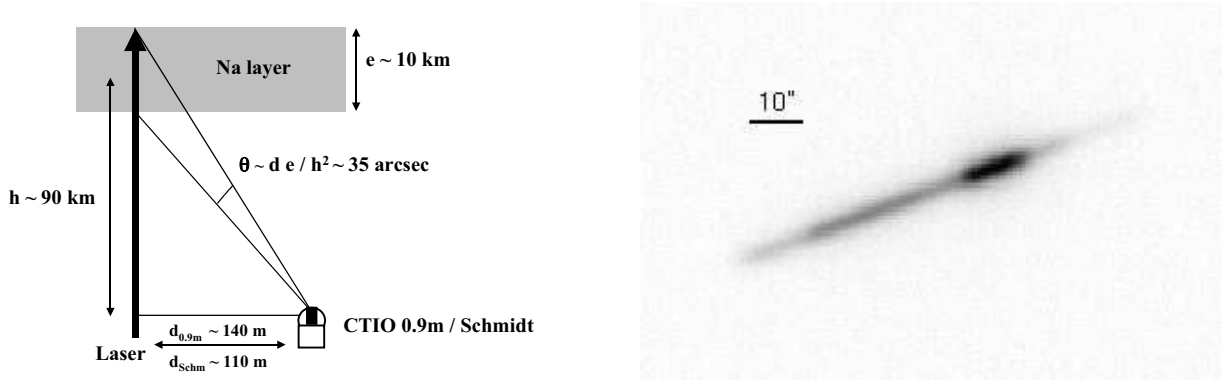

Figure 1 *Left:* Principle of mesospheric sodium monitoring with a laser, including the particular geometry used during the CTIO campaign. *Right*: Example of raw image obtained on the 0.9m telescope CCD. A sporadic layer is clearly visible on this image, which was taken at UT=04h09mn (local time 01:09am) on November 29, 2001.

The CTIO sodium monitoring campaign will provide knowledge of the sodium variability on relatively short time scales (a few seconds typically). Another technique, which relies on high-resolution spectroscopy (R=50-250k) of the sodium D1 line and proved difficult in the past due to the presence of strong water-vapor lines nearby[9], requires long exposures and prevent observation of short-lived sporadics. On February 11 (which was the first night of the sodium monitoring campaign at CTIO), September 2 and September 5 2001, we successfully monitored the sodium content above Cerro Tololo with our laser set-up while at the same time at the La Silla and Paranal Observatories, colleagues at ESO were collecting spectroscopic data at the sodium D1 line wavelength. These few hours of data overlap are expected to enable us to cross-calibrate the laser monitoring technique with the spectroscopic technique. The comparison will also give some insight on the variations of sodium abundance with latitude in the Southern hemisphere.

Run #	Dates	Total number of nights allocated per run	All weather data (for part of the night, in number of nights)	Clear weather data (for part of the night, in number of nights)
1	Feb. 11-20, 2001	10	10	9
2	May 2-11, 2001	10	6	3
3	Aug. 31-Sept. 6, 2001	7	6	4
4	Nov. 25-Dec. 1, 2001	7	7	7
5	Feb. 23-March 1, 2002	7	7	5

Table 1 CTIO sodium monitoring campaign summary.

2. SODIUM MONITORING EXPERIMENT

2.1. Set-up

The sodium monitoring experiment took place at the Cerro Tololo Inter-American Observatory (CTIO) in Chile, at a 30°S latitude. With its multiple telescopes and various utility buildings, the Cerro Tololo summit offered several possible configurations for the experiment. The CTIO 0.9m telescope was selected as the main imaging telescope because of its comparatively large collecting area enabling relatively short exposures and its low subscription factor

during bright time. Indeed, the highly monochromatic nature of the sodium streak made it possible to image the streak through a narrow-band sodium filter so that sky background was never an issue. The 0.9m telescope was also fitted with a V-filter for calibration purposes. Even though the sodium layer profile and relative altitude could be derived from a single exposure, the 0.9m telescope pointing accuracy was not sufficient to compute the sodium layer absolute altitude. We used the University of Michigan Schmidt telescope to take exposures of the sodium streak simultaneously with the 0.9m telescope and derive the sodium layer absolute altitude by triangulation. The Schmidt telescope was fitted with Na and V filters as well. The main characteristics of the 0.9m and Schmidt telescope imaging cameras are summarized in Table 2.

Characteristics	0.9m telescope	Schmidt telescope
Pixels	2048x2046	2048x2048
Plate scale	0.396"/pixel	2.32"/pixel
Field of view	13.5'x13.5'	1.3°x1.3°
Read noise	2.7-5.4 e^- depending on imaging quadrant and amplifier gain	4.8-5.0 e^- depending on imaging quadrant and amplifier gain
Filters	Na: λ=589.0nm, $\Delta\lambda$=0.6nm, T=0.67 ± 0.03 V: λ=543.8nm, $\Delta\lambda$=102.6nm, Tpeak=0.91 ± 0.03	Na: λ=589.0nm, $\Delta\lambda$=4.0nm, T=0.74 ± 0.03 V: λ=544.3nm, $\Delta\lambda$=106.0nm, Tpeak=0.88 ± 0.03

Table 2 0.9m and Schmidt telescope CCD camera parameters

The choice of the laser location resulted from a compromise between the distance to the 0.9m telescope that yielded an adequate spatial sampling across the sodium layer thickness with the 0.9m telescope CCD camera and the specific water cooling and electrical services such as a 3-phased 208V power supply required by the laser system. Consequently, the laser and its launch telescope were installed in a room adjacent to the 4m Blanco telescope cooling plant, respectively 140m and 110m away from the 0.9m and Schmidt telescopes (see Figure 1) and some 10m below the plateau where the 4m Blanco, 0.9m and Schmidt telescopes are built. Although the building we selected could not possibly be called a laser laboratory, it offered a better level of cleanliness than many other possible locations. Just as importantly, we were also given permission to cut a 1m diameter hole in the roof of that building for launching the laser beam at night. This enabled a permanent launch set-up, thus avoiding the waste of time caused by realignment of the laser launch optics at the beginning of each night. Following lessons learnt during the La Palma campaign, a removable cover blocked the hole during bad weather periods at night and during day time to protect the laser optics and electronics in the room below from possible water damage and from accumulating dust. Finally, a plastic sheet sealed the area between the launch tower and the hole in the roof in an attempt to avoid significant heat exchanges between inside and outside the building. This set-up also had the advantage to keep most flying insects out of the laser room.

The laser equipment was basically identical to the hardware used by the Imperial College for the La Palma sodium monitoring campaign[11, 12]. A large 5'x10' optical table was brought - with some effort - inside the laser room to mount the laser and launch optics. The laser system included a 6-7W multi-line argon-ion laser (Spectra Physics 2020) pumping a commercial ring-dye laser (Spectra-Physics 380D). Rhodamine 6G was used to produce the appropriate radiation at the sodium D2 line wavelength of 589.0nm. The usual set of spectrally selective elements (Lyot filter and Fabry-Perot etalon) made the laser longitudinally monomode and helped to narrow its spectrum down to an instantaneous bandwidth of about 0.5 MHz, much smaller than the 1 GHz Doppler broadening of the sodium D2 line at mesospheric temperature (~200K). The laser wavelength was precisely tuned and locked to the highest peak of the sodium D2 line using a sodium vapor cell and some feedback electronics driving a pair of Brewster galvo-plates and a piezo-actuated mirror in the dye laser cavity. A detailed description of the locking scheme is given in reference[10]. Figure 1 in the same reference also presents a schematic view of the overall optical set-up. Apart from a pair of fold mirrors and a beam sampler feeding the sodium vapor cell, the launch optical train included a X16 commercial telescope to pre-expand the laser beam diameter up to ~20mm. This pre-beam expander contained an under-sized 30μm diameter spatial filter whose purpose, besides beam clean-up, was to ensure reproducibility of the laser beam pointing on the sky after any laser cavity realignment. Once the launch optical train had been aligned and the propagation direction fixed on the sky, optimizing the laser power transmitted through the pre-beam expander allowed to bring the laser pointing back to its nominal direction whenever the dye laser output beam direction had moved. At that point, the laser beam was sent

to the sky by a custom X12 launch telescope consisting in a 100mm diameter diverging lens, a flat fold mirror to direct the beam upward, and a large 500mm diameter aspheric converging lens. The laser beam was projected ~3° off zenith at a fixed angle set by the flat fold mirror in the launch telescope. The resulting launched beam was a truncated, gaussian, ~250mm at $1/e^2$ intensity points laser beam that had initially been optimized to produce small spot sizes on the sodium layer in typical La Palma seeing conditions[11]. Spot size was optimized iteratively on the sky and on the imaging CCDs by manual focusing of the diverging lens in the launch telescope, and iterative re-focusing of the 0.9m and Schmidt telescopes.

Despite the argon-ion laser decreasing output power throughout the year and a few significant unexpected failures of the dye laser electronics, the laser system delivered 589.0nm beam powers in the ~150-350mW range at the output of the dye laser. The overall transmission coefficient through the remaining launch optics being on the order of 0.6, this translated in launched powers in the ~100-200mW range on the sky. The flux received at the 0.9m telescope were typically 60-240 photons/cm^2/s per Watt of launched laser power and out of the atmosphere, equivalent to the flux received from a 10.7 to 13 magnitude star in the V band (λ=0.55 microns, $\Delta\lambda$=0.089 microns). The laser output power was monitored in real time at a ~0.3 Hz rate so that sodium density fluctuations could be calibrated out from laser power fluctuations. Note that launched power levels were one to two orders of magnitude lower than those required to create sodium laser guide star for adaptive optics observations. In our experiment, the power level was low enough that it was safe for moving observers like aircraft pilots by current ANSI laser safety standard[14]. We did however contact the local air traffic control ahead of time before the first run and subsequently received authorization from the Chilean authorities to propagate our laser above Cerro Tololo. Finally, we used a small 8 inch Meade telescope located ~5m away from the launch telescope to detect the presence of thin cirrus that would have otherwise gone undetected and could have corrupted the mesospheric sodium abundance measurements.

2.2. Observations

There were typically three observation modes during a night. The first and most frequent observation mode had the 0.9m telescope imaging the fixed sodium streak location on the sky through its sodium filter (with tracking disabled), while the Schmidt telescope was used to image standard stars in V-band a few times a night in order to derive atmospheric transmission for that night. By not moving the 0.9m telescope, this mode made it easy to automatically acquire hundreds of successive exposures (typically 20-second) of the sodium layer. The second and third observation modes had the 0.9m and Schmidt telescopes take simultaneous exposures of the fixed sodium streak (with both telescope tracking disabled) by using a trigger cable especially installed between the two telescopes for our experiment. In normal operation, the sodium streak would appear fixed in the image while background stars drifted. The telescope CCDs had been turned appropriately so that in the so-called "drift-scan" mode instead, charges were moved on the CCD at the celestial rate of 15''/second in the east-west direction and the sodium streak drifted while the background stars now appeared fixed. This last observation mode is expected to increase the accuracy of the triangulation procedure. Simultaneous exposures of the sodium streak with both telescopes were made typically 3 to 4 times a night to yield a more accurate calibration of the sodium layer absolute altitude than what would have been obtained if using a single imaging telescope. Calibration frames such as flat fields and darks were taken throughout each run as required by standard data-reduction procedures in astronomy. We also cross-calibrated the 0.9m and Schmidt telescopes optical throughputs by simultaneously imaging standard stars in Na and V-band.

Because the Schmidt telescope had to be pointed entirely by hand, running the experiment required a minimum of three operators (one telescope operator at the 0.9m, one at the Schmidt, and one laser operator at the laser room) during the first three runs until it was made possible to control both the 0.9m and Schmidt telescopes from the Schmidt control room. Two persons sufficed during the remaining two runs (one at the laser and one at the Schmidt) as the telescope operator could now run both telescopes from the same room and be ready to go quickly point the Schmidt upstairs whenever needed.

2.3. Data quality

Binning was used to adjust the macro-pixel size of the image with the laser star width actually obtained on the sky. Together with windowing, binning enabled shorter exposures, hence higher temporal sampling of the sodium layer variations. However during clear weather and high sodium returns when signal ratios were high enough that we could have decreased the exposure time further, the temporal resolution was set by the finite read-out time of the smallest

possible region of interest (ROI) that we could define on the 0.9m CCD subarray containing the sodium steak. Elapsed time between the end of an exposure and the beginning of the next was typically 10 seconds and never went below 8 seconds. We therefore elected to use 10-second exposure times and longer, depending on the strength of the sodium return and the cloud cover at the time. During clouded nights, we increased the exposure time up to 60 seconds to observe through cirrus. Whenever weather required exposure times longer than 60 seconds, signal to noise ratios were usually so low that we stopped observing.

Although the experiment almost reached its expected temporal resolution of a few seconds, it never reached the spatial resolution limit set by the 0.9m CCD pixel size corresponding to $\Delta e \sim (\Delta\alpha \,.\, H^2) / d \sim 110$m, where $\Delta\alpha = 0.4$" is the 0.9m telescope CCD pixel size, H = 90km is the estimated sodium layer mean altitude and d = 140m is the distance between the 0.9m telescope and the laser launch site. Resolution was in practice limited by the laser spot size on the sky, typically 3 to 4" across, corresponding to spatial resolutions in the 800 to 1100m range in altitude. The sodium streak width was always much larger than the ~1" spot size expected in good seeing conditions for our close to diffraction-limited laser beam. Indeed, the laser beam quality at the output of the dye laser and the optical alignment of the launch optical train had been double-checked and were not responsible for the actual spot size obtained on the sky. The reason for this unusually large spot size was eventually traced down to the presence of four big 1m-diameter fans located just a few meters away on the side of the laser building that created strong turbulence right at the launch location. This unfortunately prevented us from taking advantage of the small 0.9m telescope CCD pixel size during good seeing nights, but the somewhat lower spatial resolution had no detrimental effect on sodium abundance measurements otherwise.

Observing efficiency suffered from the usual failure modes, including: telescope control system crashes (downtime ~10-60mn a few times per run); the laser system loosing its lock (downtime ~5-15mn at a highly variable frequency for a given night, sometimes every 15 minutes, sometimes no more than once a night); laser power dropping down to unacceptably low levels after a slow decrease for the past few hours (downtime ~10-120mn depending on whether this needed minor or major realignment); the laser system electronics taking fire (although it took us 2 days to build back-up electronics, this led to negligeable downtime as this one-time failure fortunately mostly happened during cloudy weather); and weather-related downtime due to thin to thick cirrus, fog, electrical storm and the like. However all in all we obtained enough data during each of the 5 runs with a minimum of ~15 cumulated hours of clear weather data during run #2 and a maximum of 9 full nights during run# 1 (see Table 1) that it will be possible to assess the sodium layer hourly, nightly and yearly variations eventually.

3. DATA REDUCTION

This section details how sodium measurements are derived from experimental data obtained at the telescope. Both theoretical calculations and practical data reduction techniques are presented. Because the triangulation method has not been implemented yet at this time, the section only presents sodium abundance calculations.

3.1. Sodium column density theoretical calculation

Unlike other self-calibrating laser-based techniques using LIDAR[15, 16], the proposed method relies on the theory of laser/sodium interaction and well-known sodium absorption cross-section values for linearly polarized, 0.5MHz bandwidth, longitudinally monomode continuous-wave lasers such as ours[13]. In our experiment, the laser intensities deposited on the sodium layer are more than 25 times lower than typical saturation intensity values. Besides, no significant enhancement could be observed when switching from linear to circular polarization. Therefore, the number of 589nm photons absorbed at the sodium layer simply equals:

$$N_{abs} = C_s \, \sigma \, T_{atm} \, P_{launched} \frac{\lambda_0}{h \, c} \qquad (1)$$

where C_s is the sodium column density parameter in atoms/cm^2 that we are looking for, $\sigma = 1.0\ 10^{11}$ cm^2 is the sodium D2 line peak cross section[13], T_{atm} is the (one-way) atmospheric transmission, $P_{launched}$ is the laser power launched to the sky in Watt, $\lambda_0 = 589.0\ 10^{-9}$m is the sodium D2 line wavelength, $h = 6.63\ 10^{-34}$ J.s is Planck's constant and $c = 3\ 10^8$ m/s is the speed of light. The flux of 589nm photons collected at the primary mirror of the 0.9m telescope in units of photons/cm^2/s equals:

$$F_{LGS\ @\ tel} = T_{atm} \frac{N_{abs}}{4\ \pi\ H^2} \qquad (2)$$

where $H = 90\ 10^5$cm is the estimated sodium layer mean altitude above the ground (CTIO's altitude is 2,200m above sea level). $F_{LGS\ @\ tel}$ can also be determined from the sodium layer images at the 0.9m telescope. For a natural star of V-magnitude m, the number of counts at the 0.9m telescope CCD is:

$$N_{NGS,V}(m) = K \int T_{atm}(\lambda)\ T_{opt}(\lambda)\ T_{V\ fil}(\lambda)\ \eta_{det}(\lambda)\ F_{NGS}(\lambda,m)\ d\lambda \qquad (3)$$

where $F_{NGS}(\lambda,m)$ is the natural star flux per Angstrom outside of the atmosphere in photons/cm^2/s/Å, T_{opt} is the combined transmission of all telescope and camera optics between the sky and the CCD, $T_{V\ fil}$ is the 0.9m telescope V filter transmission, η_{det} is the detector quantum efficiency, and K is the appropriate constant of proportionality to express $N_{NGS,V}$ in units of electrons or ADU per whatever unit surface and unit time. We can assume that T_{atm}, T_{opt}, and η_{det} are slowly varying with wavelength over the V band (this indeed was checked), so that equation (3) can be written:

$$N_{NGS,V}(m) = K\ T_{atm}(\lambda_0)\ T_{opt}(\lambda_0)\ \eta_{det}(\lambda_0) \int T_{V\ fil}(\lambda)\ F_{NGS}(\lambda,m)\ d\lambda \qquad (4)$$

For the simpler case of the monochromatic sodium star, equation (4) becomes:

$$N_{LGS,V} = K\ T_{atm}(\lambda_0)\ T_{opt}(\lambda_0)\ \eta_{det}(\lambda_0)\ T_{V\ fil}(\lambda_0)\ F_{LGS} \qquad (5)$$

where F_{LGS} is the flux of the sodium star outside of the atmosphere in photons/cm^2/s ($F_{LGS\ @\ tel} = T_{atm}\ F_{LGS}$).

$F_{NGS}(\lambda,m)$ is a well-known quantity in the literature. For a zero magnitude star, we find that[17]:

$$F_{NGS}(\lambda,m=0) = 3.75\ 10^{-16}\ \text{W/cm}^2/\text{Å}$$

$$\text{(i.e.) } F_{NGS}(\lambda,m=0) = \frac{3.75\ 10^{-16}}{h\ c}\ \lambda\ \text{photons/cm}^2/\text{s/Å}\ [\lambda \text{ in meters}]$$

Equation (4) therefore becomes:

$$N_{NGS,V}(m=0) = K\ T_{atm}(\lambda_0)\ T_{opt}(\lambda_0)\ \eta_{det}(\lambda_0)\ \frac{3.75\ 10^{-16}}{h\ c} \int T_{V\ fil}(\lambda)\ \lambda\ d\lambda \qquad (6)$$

We can calculate the integral in equation (6) using the 0.9m V filter transmission curve (beware that λ is in units of meters while $d\lambda$ is in units of Angstroms). Taking the ratio of $N_{LGS,V}$ in equation (5) over $N_{NGS,V}(m=0)$ in equation (6), we then derive the following expression for F_{LGS} in units of photons/cm^2/s:

$$F_{LGS} = \frac{3.67\ 10^{-19}}{h\ c} \frac{N_{LGS\ V}}{N_{NGS\ V}(m=0)} \qquad (7)$$

With $F_{LGS\ @\ tel} = T_{atm}\ F_{LGS}$, equations (1), (2) and (7) eventually lead to the desired sodium column density parameter in atoms/cm^2:

$$C_s = 3.67\ 10^{-19} \frac{4\ \pi\ H^2}{\sigma\ T_{atm}\ P_{launched}\ \lambda_0} \frac{N_{LGS\ V}}{N_{NGS\ V}(m=0)} \qquad (8)$$

3.2 Practical data reduction

To start with, all 0.9m and Schmidt telescope CCD data obtained on the sky must be cleaned up using the appropriate dark, bias, sky and/or dome flat field calibration images. Images are then corrected for cosmic rays. Extra care is taken not to introduce systematic errors when doing this standard data-reduction work. This means for instance that sub-array images (typically 600x600 in size) of the sodium streak on the 0.9m telescope are flat-fielded using corresponding dedicated subarray flat-fields whose average level has been normalized to be identical to the average level measured in the same sub-area of those full array flat field images used for standard star image reduction.

Standard star images taken throughout the campaign provide most of the necessary photometric calibration for this experiment. We used the Landolt standard star catalog[18] to image stars of brightness similar to the sodium star. Standard star images serve two purposes. First, simultaneous observations of the same standard star by both telescopes enable to calibrate the zero-point of the 0.9m telescope with its V filter against the zero-point of the Schmidt telescope with its V filter, yielding the ratio of their optical throughput in V band: $T_{0.9_V}/T_{sch_V}$. Second, observation of the same standard star throughout the night by the Schmidt telescope with its V filter yields the atmospheric extinction coefficient for that night: T_{atm}. The last set of photometric calibration is obtained by imaging the sodium star by the 0.9m telescope with its Na and V filter successively. Provided that sodium abundance has not changed between the successive exposures (true unless a fast sporadic event is developing at the time), the flux ratio of the monochromatic sodium star through both filters provides an exact calibration of the ratio of the 0.9m telescope throughputs in Na and V band: $T_{0.9_Na}/T_{0.9_V}$.

Once all data has been cleaned up and the necessary photometric calibration performed, the sodium column density parameter can be calculated using equation (8). The sodium column density cross section σ corresponding to our laser spectral format is found in the literature[13]. The sodium layer absolute altitude H will eventually be calculated using the triangulation procedure. Until this procedure is implemented, and for the results presented below, we have used an estimated value of 90 km above the ground. Note that an error of 2km on the sodium layer absolute altitude only creates a 4% uncertainty on the sodium column density parameter. The laser power projected to the sky $P_{launched}$ is derived from real-time measurements of the laser power at the laser system output, corrected from miscellaneous laser optics and launch telescope optical transmissions. To enable this calibration, the telescope control systems and the laser power meter are synchronized with Universal Time (UT) to better than ±1 second. The atmospheric transmission T_{atm} and the number of counts corresponding to a zero-magnitude star at the 0.9m telescope with its V filter $N_{NGS,V}(m=0)$ are derived from standard star calibrations as suggested above. Finally, measurements of the sodium laser flux at the 0.9m telescope through its filter, $N_{LGS,V}$, are derived from the thousands of sodium streak images taken at the 0.9m telescope through its Na filter and the separately calibrated $T_{0.9_Na}/T_{0.9_V}$ ratio.

The bulk of the data reduction work has been done through Yorick, an interpreted language for scientific computing similar to IDL. The main routine can process all sodium streak images in the following way:

- input FITS raw images, reduce them using the correct flats and bias, clean them up of cosmic rays, subtract sky background, normalize per second of exposure time;
- rotate tilted sodium streak image by pre-determined angle as measured on the image. This angle is fixed like the fixed angle of projection of the laser on the sky and the fixed position of the launch tower and the observing telescope;
- compute the integrated flux across the sodium streak width. In order to produce the results presented below, the flux was summed over 1.5 times the full width at half maximum (FWHM) which appeared to be a good compromise to include most of the flux (estimated error was 2%) and limit background noise;
- output array of reduced sodium abundance profiles versus altitude containing as many columns as images. Each row is coded over 258 elements: the first 256 elements contain the re-binned sodium profile in ADU per second, element #257 is the image number and element #258 is the decimal UT at the beginning of the exposure.

A separate routine adds two rows to the previous array, normalizes all profiles by the calibrated laser power and, using all appropriate calibrations, computes the total flux out of the atmosphere per Watt of projected laser power (stored in element #259) and the corresponding sodium column density value (stored in element #260). All sodium parameters of interests can be analyzed from there, including but not limited to: average sodium abundance over the night, extent and rate of abundance variations versus time, average sodium layer altitude variations over the night, extent and rate of altitude variations versus time, frequency and appearance rate of sporadic layers, etc.

4. PRELIMINARY RESULTS AND IMPLICATIONS FOR THE GEMINI SOUTH AO SYSTEM

So far only summer time data for runs #4 and 5 (Nov./Dec. 2001 and Feb. 2002) has been reduced. Figures 2(a) and 2(b) present the results in terms of sodium column density values plotted versus time (horizontal axis) and relative altitude (vertical axis). Results for each night are presented sequentially from bottom to top. Blanks correspond to periods when no data was recorded for one of the reasons (hardware failure/weather) presented earlier. Because the triangulation

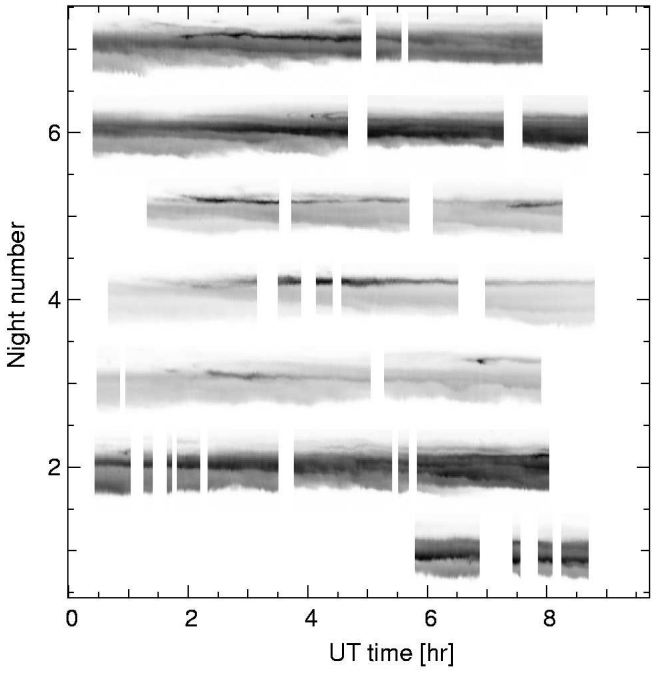

(a) Run #4

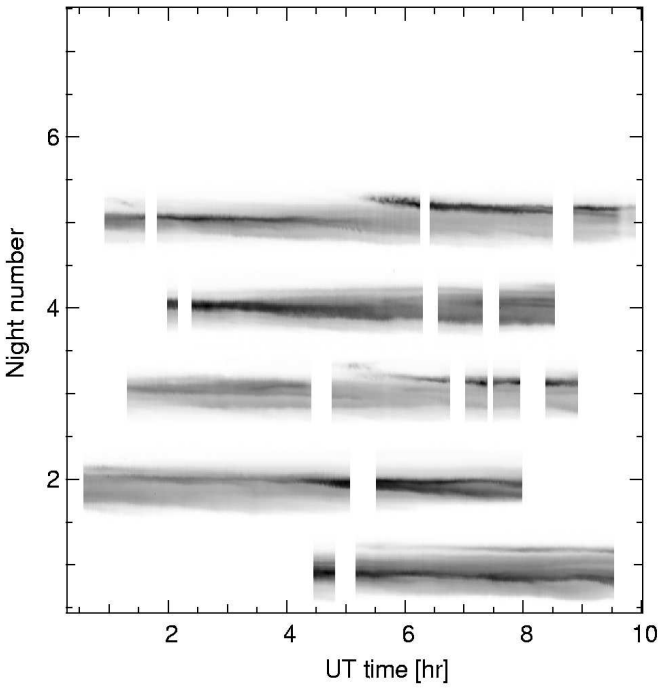

(b) Run #5

Figure 2 Example of sodium abundance vs altitude (vertical axis) and time (horizontal axis) from data obtained during run #4 (a) and #5 (b). Results are presented for each night of the runs, numbered from bottom to top, with black regions corresponding to higher sodium column densities. Profiles have been normalized separately for each night.

method has not been implemented yet, the sodium layer absolute altitude is not known to better an accuracy than a few kilometers. However, all relative altitude variations are readily available from data embedded in Figures 2(a) and 2(b).

4.1. Sodium abundance

More than any other, this parameter is crucial to the sodium LGS technique as the required laser power per beacon is almost directly proportional to the sodium column density value. For instance, a conservative sodium column density of 2 10^9 atoms/cm^2 yields a worst case power requirement per laser beacon of 15W for Gemini LGS AO observations at 45° zenith angle[19, 20]. For the planned Gemini South Multi-Conjugate Adaptive Optics (MCAO) system which will use 5 laser beacons, this could translate into laser power requirement as large as 75W if the MCAO high-level performance specifications have to be met for 45° zenith angle observations under such low sodium column densities.

Sodium abundance is expected to reach its lowest average level during summer time, possibly in November/December if we assume that Southern hemisphere mesospheric sodium exhibits the same sinusoid-like variation as presented in reference[4] for Urbana, Illinois, in the Northern hemisphere, but with a 6-month phase shift. Although no definitive conclusion can be drawn on the minimum MCAO laser power requirement before all data has been reduced, runs #4 and 5 do correspond to summer time data when the sodium content is expected to be at its lowest. In Figure 3, we plotted the histograms of all sodium column density values measured per single exposure during runs #4 and 5. These include thousands of exposures taken over 7 and 5 clear weather nights respectively. In November 2001, the histogram peaks at 3 10^9atom/cm^2 while in February 2002 it peaks at 3.5 10^9 atom/cm^2, with a mean value for both runs around 3.6 10^9 atoms/cm^2. More importantly, the minimum value rarely if ever drops below 2 10^9 atoms/cm^2 which was the conservative number used to compute the MCAO laser power requirement in references[19, 20, 21]. This seems to indicate that the Gemini MCAO laser power requirement presented at the MCAO Preliminary Design Review[19] in May 2001 stood on the conservative side. The laser power requirement will be revisited and finalized in time

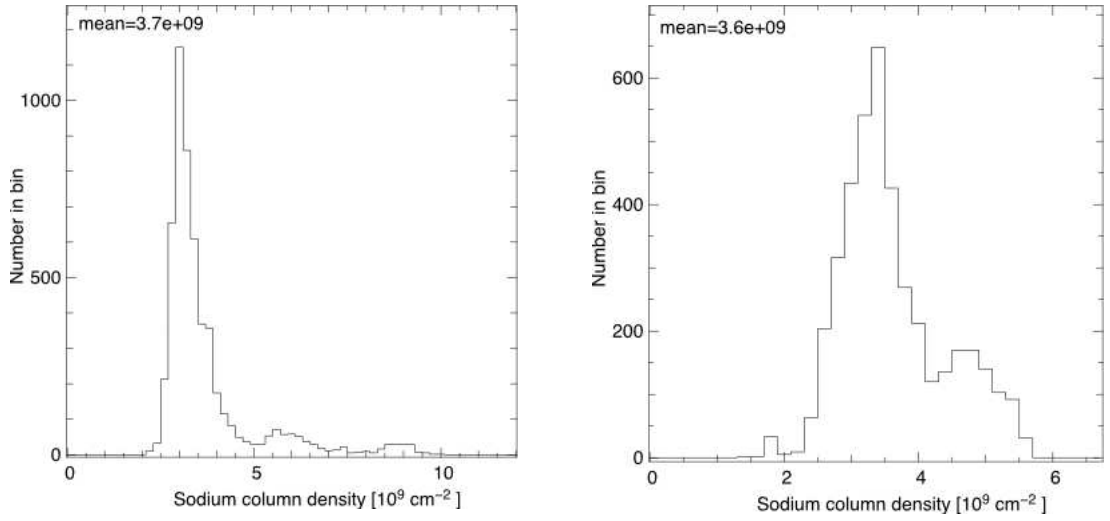

(a) Run #4 (b) Run #5

Figure 3 Histograms of sodium column density values measured throughout run #4 (a) and run #5 (b)

for the MCAO Critical Design Review, based on the complete results of the CTIO sodium monitoring campaign and the desired scientific use of the MCAO capability at Cerro Pachon.

4.2. Sodium layer altitude

The rate of mean sodium altitude variations is of prime importance for optimum removal of the focus mode in AO-corrected science images. Focus adjustments in the laser guide star path of adaptive optics systems must distinguish atmosphere-induced focus terms from slow drifts of the guide star altitude. The faster the mean sodium altitude varies, the more difficult it is to distinguish those two effects and adequately correct for them. It is currently foreseen that each laser guide star wavefront sensor (LGS WFS) of the Gemini MCAO system will be refocused every 30 seconds based on input from the MCAO imager on-instrument wavefront sensor (OIWFS) looking at a $m_V \leq 18.5$ magnitude star.

Using the data presented in Figure 2, we have plotted the RMS variations of the sodium layer mean altitude over a given time interval. A 30 second time interval yields sodium mean altitude variations of ~77m RMS and ~49m RMS with a 10% uncertainty for runs #4 and #5 respectively, which in turn correspond to ~22nm RMS and ~14nm RMS of defocus on the LGS WFS. The run #5 value is close to the LGS WFS defocus error budget of 12 nm RMS, whereas run#4 value is a factor 2 over budget. We expect the run #5 value to be closer to the yearly average as the higher value for run#4 can partly be explained by the unusually strong sporadic layer that developed at one point during the night of November 29 to November 30, 2001 (see below). Statistical results from other runs will confirm whether the sodium layer altitude variations are usually slow enough that they will not significantly degrade MCAO performance on the sky or require to lower the OIWFS update rate.

4.3. Sporadic events

The appearance of strong sporadic layers has the ability to degrade performance as well, by shifting the spot intensity centroids on the LGS WFS on short time scales. Therefore the measurement of appearance rate, thickness and intensity of sporadic layers is also important for accurate prediction of LGS AO and MCAO performance.

One of the strongest sporadic layers that we observed throughout the year developed during the night of November 29 to November 30, 2001 (see night #4 on Figure 2(a)). While the mean sodium column density was on the order of 3.6 10^9 atoms/cm^2 at the beginning of that night, a strong sporadic layer had already started to develop in the upper region of the mesosphere, bringing the mean sodium column density up to 10 10^9 atoms/cm^2 in 3 to 3.5 hours. The sporadic intensity then slowly decreased throughout the remainder of the night, bringing the sodium column density down to 6.0 atoms/cm^2 2 hours after it had peaked and 4.4 atoms/cm^2 at dawn another 2.5 hours later when we stopped observing. The detailed

statistical study of the frequency and strength of sporadic layers can only be made once all the data set has been reduced. However, from what could be seen during observations, we have the feeling that sporadic events have been much less frequent during the CTIO sodium monitoring campaign at 30°S than during the preceding campaign in La Palma at 29°N. Whether our results will eventually contribute to advance the theory according to which the mesospheric sodium sporadic layer behavior depends on latitude remains to be seen.

4. CONCLUSION

The Gemini Observatory initiated a year-long observation campaign to monitor the mesospheric sodium layer content at the Cerro Tololo Inter-American Observatory latitude (30°S) near the Gemini South telescope where a multi-laser guide star multi-conjugate adaptive optics facility is planned in the next few years. The experimental phase of the CTIO sodium monitoring campaign which took place from February 2001 to February 2002 is now complete and data-reduction is well underway. Observations yielded a total of 36 nights with usable data, among which 28 nights contain clear weather data that will provide direct information on sodium abundance mean values and variations over time and altitude. Whereas routines have been developed that yield the sodium column density values versus relative altitude and time per night of observations, the triangulation procedure to derive the sodium layer absolute altitude is still to be implemented. Among many sodium layer parameters to be derived from the sodium layer profiles, we are particularly interested in the minimum sodium column density over a year in order to set an upper limit for the Gemini South Adaptive Optics laser power requirements. Reduced data from runs #4 and #5 that took place during summer time, when sodium abundance is supposed to reach its yearly minimum, seem to indicate that the low-end sodium column density assumption of $2\ 10^9$ atoms/cm^2 that we used to calculate the MCAO laser power requirement was conservative. On another front, sodium altitude variations observed so far are on the order of what had been budgeted for the MCAO LGS WFS, and are not expected to significantly impair predicted MCAO performance.

Complete data reduction results will hopefully confirm these trends and the fact that sodium abundance variations effectively cycle over a year. Seasonal and nightly statistics of sodium density fluctuations equivalent to LGS magnitude fluctuations will give insight on conventional LGS AO and MCAO queue scheduling feasibility and efficiency. The latitude-dependence of mesospheric sodium parameters observed in the Northern hemisphere has yet to be confirmed in the Southern hemisphere, as well as a possible North/South symmetry for the mesospheric sodium abundance behavior over a year. Data gathered during the CTIO sodium monitoring campaign is also expected to contribute to test and refine existing models for the short- and long-term variations of the mesospheric sodium layer abundance and altitude over time.

ACKOWLEDGEMENTS

The Gemini Observatory is operated by the Association of Universities for Research in Astronomy, Inc., under a cooperative agreement with the NSF on behalf of the Gemini partnership: the National Science Foundation (United States), the Particle Physics and Astronomy Research Council (United Kingdom), the National Research Council (Canada), CONICYT (Chile), the Australian Research Council (Australia), CNPq (Brazil), and CONICET (Argentina).

The authors wish to thank the Cerro Tololo technical staff for their enthusiastic support of this unusual experiment in an astronomical observatory environment. They also wish to extend special thanks to the University of Michigan for granting almost unlimited access to the Schmidt telescope.

REFERENCES

1. R. Foy and A. Labeyrie, "Feasibility of adaptive telescope with laser probe", *Astron. Astrophys*., **152**, L29-L31 (1985)
2. M. Sarrazin, "Sodium beacon monitoring – A survey of related activity worldwide", http://www.eso.org/gen-fac/pubs/astclim/lgs/ (June 2001)
3. B. R. Clemesha, H. Takahashi, "Upper atmosphere research at INPE", *Advances in Space Research*, **16**, No. 5, pp. (5)141-(5)149 (1995)
4. G. C. Papen, C. S. Gardner, G. Yu, in *Adaptive Optics* Vol. 13, OSA Technical Digest Series (1996)

5. B. R. Clemesha, P. P. Batista, and D. M. Simonich, "Formation of sporadic sodium layers", *Journal of Geophysical Research*, **101**, No. A9, pp. 19,701-19,706 (Sept. 1996)
6. B. R. Clemesha, P. P. Batista and D. M. Simonich, "An evaluation of the evidence for ion recombination as a source of sporadic neutral layers in the lower thermosphere", *Advances in Space Research*., **24**, No. 5, pp. 547-556 (1999)
7. N. Ageorges, N. Hubin, R. M. Redfern, "Atmospheric sodium column density monitoring", *ESO/OSA topical meeting on Astronomy with Adaptive Optics: Present Results and Future Programs*, ESO Conference and Workshop Proc., Vol. 56, pp.3-20 (Sept. 1998)
8. C. M. M. O'Sullivan, R. M. Redfern, N. Ageorges, H.C Holstenberg., W. Hackenberg, S. Rabien, T. Ott, R. Davies, A. Eckart, "Short time-scale variability of the mesospheric sodium layer", *Experimental Astronomy,* **10**, pp. 147-156 (2000)
9. N. Ageorges, N. Hubin, "Atmospheric sodium monitor for laser guide star adaptive optics", *Astron. Astrophys. Suppl. Ser.,* **144**, pp. 533-540 (2000)
10. B. L. Ellerbroek, F. Rigaut, B. Bauman, C. Boyer, S. Browne, R. Buchroeder, J. Catone, P. Clark, C. d'Orgeville, D. Gavel, G. Herriot, M. Hunten, E. James, E. Kibblewhite, I. McKinnie, J. Murray, D. Rabaut, L. Saddlemyer, J. Sebag, J. Stillburn, J. Telle, and J.-P. Veran, "MCAO for Gemini-South", in these proceedings (2002)
11. L. Michaille, A. D. Canas, J. C. Dainty, J. Maxwell, T. Gregory, J. C. Quartel, F. C. Reavell, R. W. Wilson, and N. J. Wooder, "A laser beacon for monitoring the mesospheric sodium layer at La Palma", *Mon. Not. R. Astron. Soc.*, **318**, pp. 139-144 (2000)
12. L. Michaille, J. B. Clifford, J. C. Dainty, T. Gregory, J. C. Quartel, F. C. Reavell, R. W. Wilson, and N. J. Wooder, "Characterization of the mesospheric sodium layer at La Palma", *Mon. Not. R. Astron. Soc.,* **328**, pp. 993-1000 (2001)
13. P. Milonni, R. Q. fugate, and J. Telle, "Analysis of measured photon returns from sodium beacons", *JOSA A*, Vol. **15**, No. 1, pp. 217-233 (Jan. 1998)
14. *American National Standard for Safe Use of Lasers*, *ANSI Z136.1-2000*, Laser Institute of America, Orlando (2000)
15. G. Megie, F. Bos, J. E. Blamont, M. L. Chanin, "Simultaneous nighttime lidar measurements of atmospheric sodium and potassium", *Planetary and Space Science*, **26**, pp. 27-35 (Jan. 1978)
16. D. J. Butler, R. Davies, H. Fews, M. Redfern, N. Ageorges, W. Hackenberg, R.-R. Rohloff, S. Rabien, T. Ott, S. Hippler, "Sodium layer monitoring at Calar Alto by LIDAR", in *Adaptive Optics Systems and Technology*, SPIE Proc., Vol. 4007, pp. 358-367 (2000)
17. C. W. Allen, *Astrophysical Quantities*, Third edition, Ch. 10, p. 202, The Athlone Press Ltd, London (1976)
18. A. U. Landolt, "UBVRI photometric standard stars in the magnitude range 11.5<V<16.0 around the celestial equator", *The Astronomical Journal,* **104**, No. 1, pp. 340-371 and 436-491 (July 1992)
19. "MCAO Preliminary Design Review Documents", PDF files available on the web at http://www.gemini.edu/sciops/instruments/adaptiveOptics/AOIndex.html, in "Archive of Gemini AO related documents and presentations", "Documents" section
20. C. d'Orgeville, B. Bauman, J. Catone, B. Ellerbroek, D. Gavel, R. Buchroeder, "Gemini North and South laser guide star systems requirements and preliminary designs", in *Adaptive Optics Systems and Technology II*, SPIE Proc., Vol. 4494, pp. 302-316 (2001)
21. C. d'Orgeville, F. Rigaut and B. Ellerbroek, "LGS AO simulations and laser requirements for the Gemini LGS AO program", in *Adaptive Optics Systems and Technology*, SPIE Proc., Vol. 4007, pp. 131-141 (2000)